Proceedings of the ASME 2014 International Manufacturing Science and Engineering Conference
MSEC2014
June 9-13, 2014, Detroit, Michigan, USA

MSEC2014-4145

MULTI-OBJECTIVE PARTICLE SWARM OPTIMIZATION OF MACHINING PARAMETERS FOR END MILLING TITANIUM ALLOY TI-6AL-4V

Durul Ulutan
International Center for Automotive Research
Clemson University
Greenville, SC 29607

Abram Pleta
International Center for Automotive Research
Clemson University
Greenville, SC 29607

Laine Mears
International Center for Automotive Research
Clemson University
Greenville, SC 29607

ABSTRACT

Titanium alloy Ti-6Al-4V is a material with superior properties such as high mechanical strength, corrosion and creep resistance, and high strength-to-weight ratio, which make it an attractive material for various industries such as automotive, aerospace, power generation, and biomedical industries. However, these superior properties as well as its low thermal conductivity and chemical reactivity make it a challenge to machine Ti-6Al-4V at optimal conditions. In order to overcome this challenge, researchers constantly develop new tools and new techniques, but the extent of machining rates that can be used efficiently with those tools and techniques are usually not clear. Considering only one variable in the process and optimizing according to that variable is not sufficient because of the interactions between parameters. Also, selecting one objective function from a pool of many is not beneficial since those objectives are in conflict with one another. Therefore, this study proposes the use of a combined optimization algorithm in order to account for three major variables in end milling of Ti-6Al-4V: cutting speed, feed, and depth of cut. These variables are optimized for multiple objectives. Although it is possible to optimize the process for many different objectives, some of them are heavily correlated to each other, hence two objectives representing machinability and efficiency are selected: tool flank wear and material removal rate. The study aims to establish an optimal Pareto front of machining parameters that would optimize the conflicting outputs of the process, utilizing the multi-objective particle swarm optimization technique.

INTRODUCTION

Titanium and its alloys such as Ti-6Al-4V have high mechanical strength and low density, which make it a great candidate of material for various industries with lightweight material focus. However, due to high mechanical strength, titanium alloys also require high machining force that prevents from achieving good surface finishes as well as inducing high tool wear. In addition, due to its low thermal conductivity, the heat generated in the friction zone between the chip and the tool rake face while machining these alloys cannot be dissipated sufficiently and hence causes high tool wear. Titanium also has high chemical reactivity with many tool materials. Therefore, due to its high strength, low thermal conductivity, and high chemical reactivity with tool materials, it is accepted to be a difficult-to-machine (low machinability) material [1-6]. Its low machinability is usually observed as high machining forces and spindle power consumption. Due to the increased machining forces, the tool flank wears out rapidly. As a result, frequent tool change is required, which increases the cost of tooling and reduces productivity and efficiency. Moreover, the surface quality of the end product deteriorates, causing surface problems such as surface roughness, tensile residual stresses, machining-affected zone thickness, and surface microhardness.

One way to improve these criteria of machinability is to use less aggressive machining conditions by decreasing cutting speed, feed, and depth of cut. Usually, these parameters are reduced to achieve the surface quality required by the process since the tool wear decreases. However, decreasing these parameters also decreases the material removal rate (*MRR*), which is an indication of the process efficiency. If the process is running at low *MRR*, required throughput for a certain

product may not be met, so it cannot be reduced beyond the limits of the process.

Therefore, these industrial objectives (machinability and efficiency) are in conflict with each other, and finding the optimal set of these objectives is necessary. Although it is not possible to find a unique optimal solution that minimizes both, it is feasible to suggest a Pareto-optimal set of solutions. For these solutions, it would not be possible to improve one of the objective functions without sacrificing the optimality of the other objective function.

This study presents a multi-objective optimization methodology to find such a Pareto-optimal front that defines the optimal set of solutions using Particle Swarm Optimization (PSO) technique. First, a full design of experiments study with three factors at three levels each was conducted, and the resultant force, spindle power consumption, and tool flank wear were measured. Then, the outputs were analyzed and it was found that the three measured outputs are highly correlated with each other. Therefore, one of these outputs (tool flank wear) was chosen, and a best-fit curve using a regression model was fit into the data. By this curve and the equation for material removal rate, a three-input two-output multi-objective optimization scheme was built and Particle Swarm Optimization was employed to create the Pareto-optimal front in the objective function space.

The experiments in this study cover a wide range of machining variables with mild as well as aggressive cutting conditions. Therefore, using the findings of this research, machining parameters for Ti-6Al-4V can be selected in such a fashion that required surface quality can be achieved at minimal tooling cost, while not compromising from the efficiency of the process. These variables can be selected according to the process requirements by the machine operator, and the expected compromise from each objective will be known prior to machining.

EXPERIMENTAL SETUP

For this study, rectangular blocks of Ti-6Al-4V with dimensions of 80mm x 60mm x 25mm were prepared. An indexable Sandvik tool with a diameter of 15.875mm was with two inserts of type R390-11T308M-PM 1030, which tungsten carbide inserts with multi-layer TiAlN coating via physical vapor deposition (PVD). Flood coolant was used on the tool-workpiece contact zone throughout the duration of testing. Parameters used for machining were significantly aggressive than those found in the literature [7-9], and these parameters can be found in

TABLE 1: . A full design of experiments was employed with three factors (cutting speed, feed, depth of cut) and three levels of each factor, and two replications of each test were conducted to ensure the reliability of the data, particularly at more aggressive conditions. A constant width of cut of 9.5mm was used, which corresponds to 60% engagement of the tool, a maximum limit defined by the tool manufacturer.

Tests were completed on an OKUMA ACE center MB-46VAE 3-axis CNC vertical milling machine, forces were measured using a Kistler 3-component dynamometer in three orthogonal directions, and the spindle power consumption was measured using Caron Engineering equipment and software. After each test, the inserts were changed with fresh ones, and the used ones were tested for tool flank wear using an Olympus SZX12 optical microscope.

TABLE 1: MACHINING PARAMETERS USED IN TESTING

	Cutting Speed	Feed	Depth of Cut
Test #	[m/min]	[mm/rev]	[mm]
1	50	0.1	0.5
2	150	0.1	0.5
3	250	0.1	0.5
4	50	0.3	0.5
5	150	0.3	0.5
6	250	0.3	0.5
7	50	0.5	0.5
8	150	0.5	0.5
9	250	0.5	0.5
10	50	0.1	1
11	150	0.1	1
12	250	0.1	1
13	50	0.3	1
14	150	0.3	1
15	250	0.3	1
16	50	0.5	1
17	150	0.5	1
18	250	0.5	1
19	50	0.1	1.5
20	150	0.1	1.5
21	250	0.1	1.5
22	50	0.3	1.5
23	150	0.3	1.5
24	250	0.3	1.5
25	50	0.5	1.5
26	150	0.5	1.5
27	250	0.5	1.5

ANALYSIS

After the measurements were taken, they were analyzed together. First the resultant force for each test was calculated by doing a vector sum of the three components of the measured machining forces. Also, average tool flank wear measurements from the two inserts of each test were averaged, and the resultant force, power, and average tool flank wear values were also averaged over the replications. Since no significant difference was observed between replications, two runs of each test were found to be satisfactory.

Using highly correlated objectives can be detrimental to the working methodology of the optimization algorithm, and there is not additional information when one of the objectives is highly correlated to another. Therefore, a correlation analysis

was conducted between the measured outputs. It was found that all three were highly correlated to each other. Spindle power consumption is proportional to the orthogonal component of the machining force, which is the reason that the resultant force and power consumption are highly correlated (R^2=0.87). Also, it is known that when the machining forces are high, tool flank wear increases due to increased mechanical loading. This was also shown with the high correlation between the two measured outputs (R^2=0.83). Hence, only one of these outputs was selected. The reason for selecting tool wear was that it is the direct indicator of process failure, whereas the other two cannot directly show that the process have failed. One can use the resultant force or spindle power consumption for the same purpose, if the limiting constraint is the capacity of the milling machine. However, with a highly capable milling machine, the process failure modes were determined to be high tool flank wear (tool failure) and low material removal rate (low efficiency). Therefore, these two were used in the multi objective optimization model. The results of the experiments in terms of these two objectives (as well as the converted parameter MRR^{-1}) are presented in TABLE 2.

TABLE 2: OUTPUTS OF THE EXPERIMENTS

	Tool Wear	MRR	MRR^{-1}
Test #	[µm]	[mm^3/s]	[$s/1000mm^3$]
1	61	8	126
2	50	16	63
3	56	24	42
4	62	24	42
5	61	48	21
6	71	71	14
7	55	40	25
8	68	79	13
9	71	119	8
10	75	24	42
11	69	48	21
12	74	71	14
13	83	71	14
14	116	143	7
15	83	214	5
16	74	119	8
17	123	238	4
18	123	357	3
19	68	40	25
20	60	79	13
21	58	119	8
22	77	119	8
23	87	238	4
24	91	357	3
25	79	198	5
26	198	397	3
27	288	595	2

After determining the objective functions, it is essential to find or construct equations that relate the decision variables to objective functions. Material removal rate is already directly related to the three decision variables using Eq. (1), where *MRR* is the material removal rate, v_c is the cutting speed, f is the feed, a_p is the depth of cut, D_t is the diameter of the tool (fixed at 15.875mm), and w is the width of cut (fixed at 9.5mm). However, since material removal rate needs to be maximized, this study uses the inverse of this objective (MRR^{-1}). On the other hand, no direct relation exists between the decision variables and tool flank wear. Thus, it is constructed through a regression analysis. Since the interactions between the machining parameters are also effective on tool wear, all second order terms (interaction and square terms) are considered in the original equation. However, the p-values for the square terms are very high (p>0.6), which suggests that those terms do not contribute in the regression significantly. On the other hand, all the first order terms as well as the interaction terms has p-values less than 0.05, so their effects are significant in the regression. Therefore, the regression equation is constructed using only the first order and interaction terms (Eq. 2), where *VB* is the tool flank wear, and β_i are the regression coefficients given in TABLE 3: . This equation has an R^2 value of 0.81, which means that the model represents 81% of the variability in the data.

$$MRR = \frac{v_c f a_p w}{\pi D_t} \quad (1)$$

$$VB = \beta_0 + \beta_1 v_c + \beta_2 f + \beta_3 a_p + \beta_4 v_c f + \beta_5 v_c a_p + \beta_6 f a_p \quad (2)$$

TABLE 3: REGRESSION COEFFICIENTS FOR TOOL FLANK WEAR (EQ. 2)

β_0	β_1	β_2	β_3	β_4	β_5	β_6
163.8	-0.511	-320.6	89.53	1.467	0.3217	241.7

MODELING

In order to understand how each decision variable can be used to optimize the objectives, a multi-objective optimization model is constructed. In this model, the three decision variables were the cutting speed, feed, and depth of cut, and they were bounded by the minimum and maximum values they took in the experimental design. The two objective functions (MRR^{-1} and *VB*) were bounded only by the non-negativity constraint, as they cannot take negative values. If such a case occurs, the model reiterates until a valid solution is found. The objective of the multi-objective optimization model is to find the solutions that cannot be further improved, and the combination of those solutions represents the Pareto-optimal front. Unlike some methods that combine objectives through weighing, in multi-objective optimization, the purpose is to construct the Pareto-optimal front rather than suggesting a single optimum.

For the optimization purpose, Particle Swarm Optimization method is utilized. This method is an evolutionary computation

method similar to genetic algorithms. As detailed by Parsopóulos and Vrahatis [10], finding the Pareto-optimal front in the multi-objective optimization problems is important, and Particle Swarm Optimization is a very effective method in capturing the Pareto front instead of having to apply a weighted aggregation technique. Particle Swarm Optimization has found use in many different complex systems where quick solutions are essential, such as machining processes [11-15]. In both genetic algorithms and particle swarm optimization, a random set of predetermined amount of particles are initialized in the decision variable space and the objective functions corresponding to those particles are calculated using equations like Eq. (1-2). However, in genetic algorithms, these particles mutate or die in subsequent iterations, whereas in particle swarm optimization, particles do not mutate or die. Instead, their velocities change over iterations (analogous to generations in genetic algorithms), and random disturbances to particle velocity (and hence position) ensure that local minima are handled.

In the particle swarm optimization method, each particle has a random initial position and velocity. This randomness ensures that all of the decision variable space can be searched for possible solutions. At each iteration, particle's position and velocity are updated using Eq. (3-4), where i is the particle number, n is the iteration number, x is the position and v is the velocity of each particle at each iteration, K is a dynamic velocity factor, a_1 and a_2 are acceleration terms that can be found using Eq. (5), p_i is the best observed position of the particle i until that iteration based on objective function values (personal best), g is the best position over all particles observed until that iteration (global best), δ' and δ_j are random numbers between [-1, 1], and c_j are predetermined acceleration constants. The first term in Eq. (4) pulls the particles toward their personal best; the second term pull them toward the global best; and the last term δ' ensures that even if everything else vanishes (if the particle is at the global best), the particle will have a random stochastic disturbance to avoid local minima and keep searching for possible improved solutions. The positions and velocities are defined as vectors, so each particle will have a position and a velocity component in all direction in the decision variable space. Also, in the beginning of iterations, the K factor is defined to be bigger, since it is more beneficial for the particles to move around in the decision variable space as much as possible. However, with progressing iterations, its value decreases, since the particles are assumed to have nearly settled to their final states.

$$x_i^{n+1} = x_i^n + K v_i^{n+1} \quad (3)$$

$$v_i^{n+1} = a_1(p_i - x_i^n) + a_2(g - x_i^n) + \delta' \quad (4)$$

$$a_j = c_j \delta_j, \qquad j=1, 2 \quad (5)$$

After the positions and velocities of all particles are calculated at each iteration, they are checked for bounds. Just like positions are bounded by the experimental design minima and maxima, velocities are also bounded by a predetermined value to avoid jerky movement of particles or divergence of the algorithm. Then, the objective functions are calculated using Eq. (1-2), and personal and global best values are checked. If any particle has an objective value lower than its personal best, it is updated. If any of the personal bests are better than the global best, then the global best is updated. Also, all personal bests are compared in each step, so that their "non-dominance" is checked. If a particle best has higher values for all objective functions compared to another particle, that particle is said to be dominated. This means that there exists another particle, which can improve the solution of the dominated particle in at least one objective function without sacrificing from the other objective function. These particles keep moving around to find a better solution, but are not represented in the Pareto-optimal front. The iterations stop at a predetermined number, or if there is no change in the personal or global bests for consequent iterations.

RESULTS

The multi-objective particle swarm optimization algorithm is programmed using MATLAB, and a population size of 1000 is selected to ensure that the complete decision variable space is represented in the model. In the cases of higher maximum number of iterations, the algorithm stopped approximately at 100 iterations, so it is selected as 100. Even with such high number of particles, the simulation finishes in less than 3 minutes on a computer with Dual Core processor, supporting that this method provides quick solutions.

Two objective functions are shown in FIGURE 1, where tool wear is in μm and the inverse of material removal rate is in seconds per 1000 mm^3 for ease of display purposes. This figure shows the end of the simulations (after 100 iterations with 1000 particles). Only the particles that are non-dominated are shown here, at their personal best states. In order to make it easy to track each particle, one that has the lowest tool wear but also the lowest material removal rate (highest MRR^{-1}) is shown with blue, the particle that has the highest *MRR* but also the highest tool wear is shown with red. The particles that are in between have decreasing tone of blue and increasing tone of red with increasing tool wear (and increasing *MRR*), therefore creating a Pareto front running from blue to purple to red.

The decision variable space consists of three factors, therefore a full representation requires a three-dimensional figure. However, in order to make it easy to observe trends, two-dimensional graphs are shown in all three decision variable space. FIGURE 2 shows the decision variable space in terms of feed and cutting speed, whereas FIGURE 3 shows it for depth of cut and speed, and FIGURE 4 shows it for depth of cut and feed. From these figures, it can be concluded that the particles gathered at high depth of cut, whereas medium to high cutting speeds and low to medium feeds are dominant in the decision variable space. It is also observed that lowest cutting speed particles are the bluest, which favours low tool wear but compromises from material removal rate, whereas highest feed particles are the reddest,

which favours high material removal rate but compromises from tool wear.

The mildest conditions (lowest speed, feed, and depth of cut) do not even show on the graphs, as this condition is not beneficial in any way (*i.e.* it cannot create a dominant solution). Similarly, the most aggressive conditions cause too high tool wear, so they cannot constitute a dominant solution either. The main takeaway from these graphs is that the Pareto-optimal front can be created for these two conflicting objective functions, and depending on the needs of the process, the machine operator can make the decision of parameter selection.

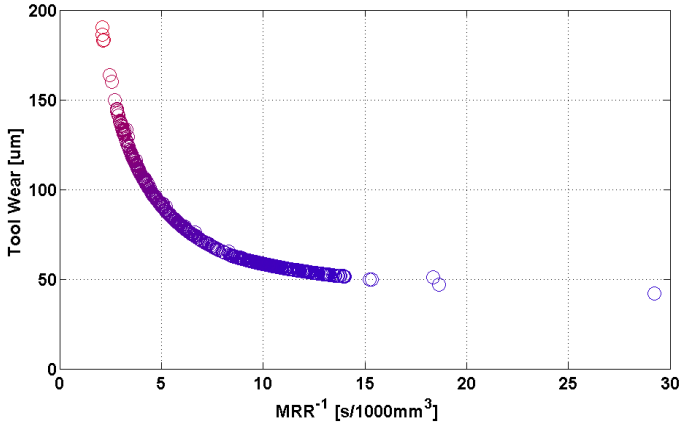

FIGURE 1: REPRESENTATION OF PARTICLES IN THE OBJECTIVE FUNCTION SPACE AT THE END OF THE SIMULATION

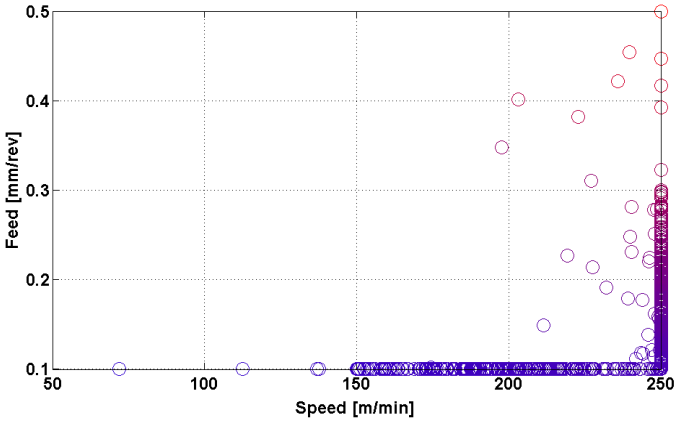

FIGURE 2: REPRESENTATION OF PARTICLES IN THE DECISION VARIABLE SPACE (FEED VS. SPEED)

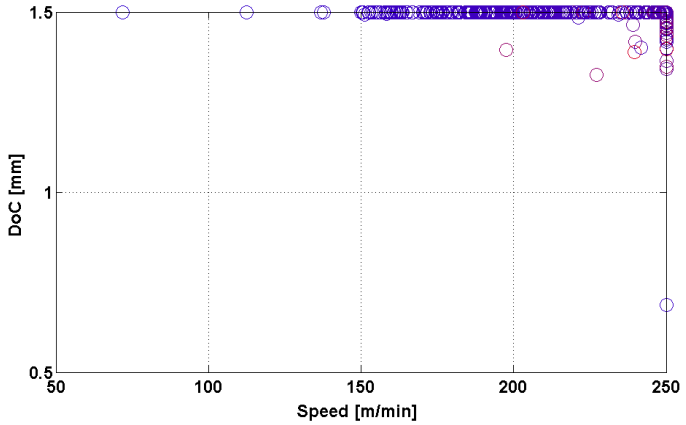

FIGURE 3: REPRESENTATION OF PARTICLES IN THE DECISION VARIABLE SPACE (DEPTH OF CUT VS. SPEED)

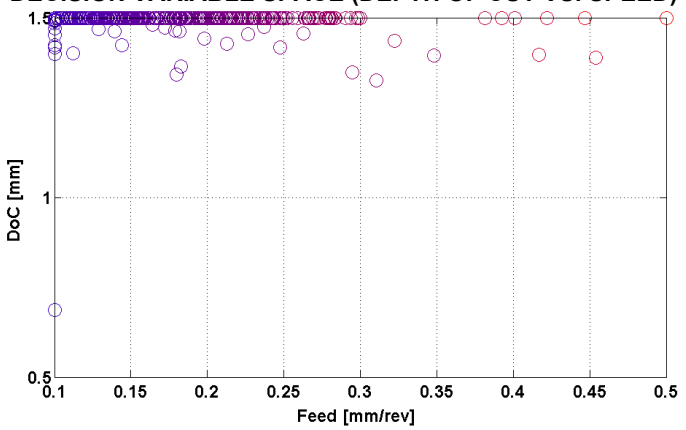

FIGURE 4: REPRESENTATION OF PARTICLES IN THE DECISION VARIABLE SPACE (DEPTH OF CUT VS. FEED)

CONCLUSIONS

This study aimed to propose a multi-objective optimization algorithm to tackle the issue of conflicting objectives in machining titanium alloy Ti-6Al-4V. Although this was a preliminary study of what can be an extended search for the correct set of parameters to machine Ti-6Al-4V, the findings are very promising.

- A full factorial experimental design was conducted with three factors (cutting speed, feed, depth of cut) at three levels each.
- Machining forces in three directions, spindle power consumption, and average tool flank wear were measured and analysed.
- High correlations between the measured outputs were revealed. As a result of this, only tool flank wear was selected for investigations, since it is the variable that indicates process failure directly. In addition, material removal rate was investigated as the conflicting objective function to represent efficiency of the machining process.
- Particle Swarm Optimization method was used to build a multi-objective optimization model based on

the regression fit to the results for tool flank wear and the calculated value of material removal rate.

- As a result of the multi-objective particle swarm optimization model, a Pareto-optimal front was found without non-dominant solutions. It was observed that particles mostly aligned with high depth of cut, medium to high cutting speed, and low to medium feed. Moreover, it was concluded that feed increase moved the particles on the Pareto-optimal front toward high tool wear, whereas speed decrease moved them toward high material removal rate.

ACKNOWLEDGMENTS

The authors wish to thank GE Power & Water for support of this work.

REFERENCES

[1] Ulutan, D., and Özel, T., 2011, "Machining Induced Surface Integrity in Titanium and Nickel Alloys: A Review," International Journal of Machine Tools and Manufacture, 51, pp. 250-280.

[2] Pervaiz, S., Deiab, I., and Darras, B., 2013, "Power Consumption and Tool Wear Assessment when Machining Titanium Alloys," International Journal of Precision Engineering and Manufacturing, 14, pp. 925-936.

[3] Yang, X., and Liu, C.R., 1999, "Machining Titanium and Its Alloys," Machining Science and Technology 3(1), pp. 107-139.

[4] Rahman, M., Wang, Z.G., and Wong, Y.S., 2006, "A Review on High-Speed Machining of Titanium Alloys," JSME International Journal Series C Mechanical Systems, Machine Elements and Manufacturing 49(1), pp. 11-20.

[5] M'Saoubi, R., Outeiro, J.C., Chandrasekaran, H., Dillon Jr., O.W., and Jawahir, I.S., 2008, "A Review of Surface Integrity in Machining and Its Impact on Functional Performance and Life of Machined Products," International Journal of Sustainable Manufacturing, 1, pp. 203-236.

[6] Rahman, M., Wong, Y.S., and Zareena. A.R., 2003, "Machinability of Titanium Alloys," JSME International Journal Series C Mechanical Systems, Machine Elements and Manufacturing 46(1), pp. 107-115.

[7] Pervaiz, S., Deiab, I., and Darras, B., 2013, "Power Consumption and Tool Wear Assessment When Machining Titanium Alloys," International Journal of Precision Engineering and Manufacturing, 14, pp. 925-936.

[8] Italo Sette Antonialli, A., Eduardo Diniz, A., and Pederiva, R., 2010, "Vibration Analysis of Cutting Force in Titanium Alloy Milling," International Journal of Machine Tools and Manufacture, 50, pp. 65-74.

[9] Sima, M., Ulutan, D., and Özel, T., 2011, "Effects of Tool Micro-Geometry and Coatings in Turning of Ti-6Al-4V Titanium Alloy," *Transactions of the North American Manufacturing Research Institution of SME*, 39, pp. 395-402.

[10] Parsopóulos, K.E., and Vrahatis, M.N., 2002, "Particle Swarm Optimization Method in Multiobjective Problems," *Proceedings of the ACM Symposium on Applied Computing*, Madrid, Spain, pp. 603-607.

[11] Hu, X., and Eberhart, R., 2002, "Multiobjective Optimization Using Dynamic Neighborhood Particle Swarm Optimization." *Proceedings of the 2002 Congress on Evolutionary Computation*, Honolulu, HI, pp. 1677-1681.

[12] Coello Coello, C.A., and Becerra, R.L., 2009, "Evolutionary Multiobjective Optimization in Materials Science and Engineering." Materials and Manufacturing Processes, 24(2), pp. 119-129.

[13] Chakraborti, N., Jayakanth, R., Das, S., Calisir, E.A., and Erkoc, S., 2007, "Evolutionary and Genetic Algorithms Applied to Li+C System: Calculations Using Differential Evolution and Particle Swarm Algorithm." Journal of Phase Equilibria and Diffusion, 28(2), pp. 140-149.

[14] Thepsonthi, T., and Özel, T., 2012, "Multi-Objective Process Optimization for Micro-end Milling of Ti-6Al-4V Titanium Alloy," International Journal of Advanced Manufacturing Technology, 63, pp. 9-12.

[15] Ulutan, D., and Özel, T., 2013, "Multiobjective Optimization of Experimental and Simulated Residual Stresses in Turning of Nickel-Alloy IN-100," Materials and Manufacturing Processes, 28, pp. 835-841.